

Enhancing the accuracy of virtual screening: molecular dynamics with quantum-refined force fields

Alessandro Curioni*, Tiziana Mordasini & Wanda Andreoni
IBM Research, Zurich Research Laboratory, CH-8803 Rüschlikon, Switzerland

Received 30 April 2004; accepted in revised form 13 December 2004
© Springer 2005

Key words: binding affinity, binding energy, lead optimization, molecular dynamics, protein–ligand interaction, scoring, structure-based drug design, virtual screening

Summary

A methodology aimed at improving the accuracy of current docking–scoring procedures is proposed, and validated through detailed tests of its performance in predicting the activity of HIV-1 protease inhibitors. This methodology is based on molecular dynamics simulations using a force field whose effective charges are refined by means of a novel procedure that relies on quantum-mechanical calculations and preserves the internal consistency of the parameterization scheme.

Introduction

Lead optimization is a crucial step in the complex process of drug design. The parallel strategies used to fine-tune the bioactivity of leads include computer modeling and simulations, which are playing an increasingly important role. For example, methods such as QSAR, high-throughput docking and scoring methods are currently in widespread use. Still, improvements are needed in each of the different steps required in rational drug design and at different levels of performance, in terms of both efficiency and reliability. The increasing availability of protein structures, which are targets of the molecular drug, represents a great step forward for rational drug design [1] because the identification of active sites has become possible. However, also in structure-based drug design, the need is felt for more accurate, robust and flexible computational approaches, which go beyond the identification of probable conformations of the ligand–protein

complex and are able to predict ligand–protein binding affinities with higher precision than today’s methods (see e.g. [2, 3]). Two major bottlenecks are the limited accuracy of the force fields used to describe the ligand–protein complexes and the inability of exploring a sufficiently large set of possible binding configurations. In this paper, we propose a novel and general methodology that allows one to significantly enhance the performance of the force field by improving the parameterization of the electrostatic interactions, and to combine it with classical molecular dynamics (MD) for the sampling of the conformational space. The novelty of our method consists in refining the atomic charges – on the grounds of *ab initio* calculations based on density functional theory (DFT) [4, 5] – subject to specific restraints, in such a way that their new values do not disrupt the consistency of the original parameterization and thus its reliability. This procedure leads to a new consistent interaction scheme that we call quantum-refined force field (QRFF).

Indeed, given that in general the original optimization of the force field parameters is global, i.e.

*To whom correspondence should be addressed. Fax: +41-1-724-8962; E-mail: cur@zurich.ibm.com

made simultaneously for all parameters, a partial replacement according to standard formulations [6] could disrupt the validity of the entire scheme. This is especially dramatic for force fields using the united-atom model and the description of interactions, such as hydrogen bonds, that result from a delicate balance of electrostatic and dispersion forces and are critical for a sensible MD-driven simulation of the evolution of the real system. The proposed refinement, once applied to a force field tailored to provide an accurate description of the global physico-chemical behavior of the receptor in solution, guarantees applicability to complexes with diverse ligands.

Application of the concept of a QRFF proved useful in our study of the binding of progesterone with its human receptor [7] and led to a significantly better understanding. Here we give a detailed explanation of the method and explore its validity for the quantitative prediction of ligand–protein affinities. In particular, we test its performance on HIV-1 protease inhibitors, starting from an educated guess of the binding conformation and the experimental knowledge of the structure of the target [8].

We select a set of inhibitors for which experimental data of activities *in vitro* are available and predictions have been made based on the inhibitor–enzyme interaction energies obtained from molecular mechanics calculations in the gas phase [8]. The first and main step of our work concerns the refinement of the parameterization of the ligands and the calculation of interaction energies from averaging over the configurations generated by MD simulations at room temperature. Further steps were made to investigate whether much more computer-intensive and hence expensive calculations are necessary for the improvement of the predictions: on one side we extended the quantum refinement of the effective charges relative to the atoms of the residues surrounding the active site, and on the other hand computed free energy differences and used these rather than interaction energies to obtain ligand–protein affinities.

Method: QRFF

We have used classical MD simulations to sample the conformations of the ligand–protein complexes and determine the ligand-binding interaction

energies. Calculations were performed with the GROMOS96 package and the united-atom GROMOS force field (43A1) [9] for the description of the receptor and the associated SPC water model [10]. The parameterization of this force field is well established for the study of proteins, namely their structure, dynamics and thermodynamic properties. Therefore, the fundamental step to ameliorate the description of the interaction is suitable modification of the parameters used for the ligand. Here we focus on improving the electrostatic interaction and on developing a new procedure that suitably modifies the values of the effective atomic charges associated with the atoms of a given ligand and/or the atoms of the active site.

First, energy minimization is performed to optimize the structure of the ligand interacting with the protein, using the unrefined GROMOS force field. Then the ligand, kept in the binding conformation, is isolated and its electrostatic potential is calculated from first principles with CPMD [5]. To determine the *ab initio* electrostatic potential at the active site, the structure we chose as representative was the initial configuration of all our MD simulations (see the section Preparation of initial systems) after energy minimization in water.

The *ab initio* scheme is based on DFT [4], norm-conserving, angular-momentum-dependent pseudopotentials [11] and a plane-wave basis set for the expansion of the electronic wave functions up to a cutoff that ensures convergence in the valence space. This latter feature increases the accuracy to the computational scheme and avoids the uncontrolled drawbacks of commonly used representations based on localized basis sets [12]. In particular, the gradient-corrected exchange–correlation energy functionals introduced by Becke [13] and Lee et al. [14] are used. The *ab initio* electrostatic potential thus obtained is fitted with a distribution of effective atomic charges whose values are determined subjected to an appropriate restraint such as to maintain consistency with the remainder of the parameterization. Specifically, the function to be minimized is

$$X^2 = X_{\text{esp}}^2 + X_{\text{res}}^2, \quad (1a)$$

with

$$X_{\text{esp}}^2 = \sum_i (V_i' - V_i)^2 \quad (1b)$$

and

$$X_{\text{res}}^2 = \sum_j a_j (q_j - q_{0,j})^2, \quad (1c)$$

where V_i is the value of the *ab initio* electrostatic potential on the i th point of the 3D grid (the same real-space grid as used in CPMD to describe the electron density, excluding the points inside the van der Waals spheres centered on the atomic positions), V'_i is the potential due to the point charge distribution, $q_{0,j}$ is the original GROMOS effective charge associated with the j th atom, q_j is the refined value to be determined, and the a_j 's are atom-dependent parameters representing the strength of the restraints. For the sake of simplicity, in the application to HIV-1 protease inhibitors we have adopted the same a_j constant for all the explicit atoms and ascribed a number that is orders-of-magnitude higher to the hydrogens modeled as united atoms. The a_j values have then been adjusted in such a way that the relative error introduced by the restraint was at most 5% of the error of the original fitting. Note that for $q_{0,j} = 0$ our formulation reduces to that introduced in [12] and which has become part of the standard parameterization of the AMBER package [15]. This latter choice of the restraint avoids unphysical fluctuations of the fitted charges, which was the concern of [12]. On the other hand, our choice is dictated by a different philosophy, namely it is aimed at avoiding an inconsistency of the modified charges with the remainder of the force field.

Application to HIV-1 protease inhibitors

Preparation of initial systems

Starting coordinates were taken from the X-ray structure of the acetylpepstatin-inhibited HIV-1 protease dimer [16] (PDB entry 5HVP). All (170) X-ray water molecules present in the crystallographic structure were retained. Following previous modeling [8], the catalytic Asp25 was protonated at O_δ .

The HIV-1 protease inhibitors we consider here (see Tables 1 and 2) were taken from [8]: 30 out of 33 for the training set and six for the

prediction set¹ with the addition of indinavir sulphate – a drug currently in clinical use, and better known by its trade name Crixivan [17]. Each ligand was first docked into the binding site manually in an orientation similar to that known from the X-ray structure of similar complexes. Then its atomic coordinates were optimized via a local energy minimization by keeping the HIV dimer fixed in the crystallographic positions. Then the complex was solvated in a cubic box, the size of which allowed at least 0.9 nm between the solute and the box wall. A second local energy minimization was applied to the entire system corresponding to a total of 53,406 atoms including 17,149 explicit SPC water molecules. In this calculation and subsequent MD simulations, periodic boundary conditions were applied. Non-bonded interactions were evaluated using the twin-range cut-off method, and electrostatic interactions beyond 1.4 nm were approximated with a Poisson–Boltzmann generalized reaction field term.

MD simulations

For each ligand–protein complex in the aqueous solution, three sets of MD runs were carried out with different prescriptions for the effective atomic charges of the ligand: (i) GROMOS 43A1 values, quantum-refined values obtained according to Equation (1) for (ii) the initial structure [phase I] and (iii) the conformation corresponding to the final snapshot of the runs with the parametrization (ii) [phase II].

After the initial preparation as described above, the system was equilibrated by performing a 10 ps MD simulation at constant volume with the solute in fixed geometry followed by 10 ps at constant pressure. Afterwards the solute was allowed to move freely and the temperature was slowly raised from 50 to 300 K with intervals of 5 ps simulations. When the temperature had reached 300 K, further 30 ps MD runs at constant temperature and pressure were carried out. Subsequent to this

¹For three compounds (numbers 7, 10, 14 in the list of [8], p. 309) the set of GROMOS parameters was incomplete. For the prediction set 6 out of 16 compounds were chosen, due to the lack of proper internal parameters in the original force fields. Moreover we tried to include some of the compounds that were showing the largest deviation between predicted and observed pIC_{50} in [8] (inhibitors number 36, 38, 49, 50).

Table 1. Interaction energies E_{inter} (kcal/mol) (ligand–protein plus ligand–water) calculated for the training set with different parametrizations (see text) and corresponding values of pIC_{50} .

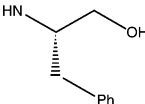
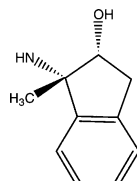
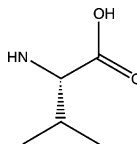
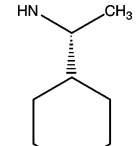
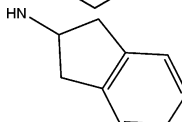
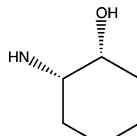
Inhibitor no.	R1	R2	R3	R4	$[E_{\text{inter}}]$ pIC ₅₀ (calc.)			Exp. pIC ₅₀
					GROMOS	QRFF(I)	QRFF(II)	
30				NHCH ₂ C ₆ H ₁₁	[−115.3] 7.07*	[−112.0] 6.88*	[−110.9] 6.39*	4.5229
11	H	H	H		[−117.2] 7.25*	[−120.3] 7.75*	[−123.6] 7.76*	5.5325
22					[−131.6] 8.66*	[−122.6] 7.99*	[−127.0] 8.12*	6.1612
25					[−128.3] 8.33	[−116.1] 7.31	[−123.8] 7.78	6.6728
23					[−120.5] 7.57	[−121.0] 7.82	[−121.8] 7.56	6.7932
32					[−113.8] 6.91	[−122.9] 8.02	[−123.8] 7.78	6.8356
31					[−127.5] 8.26	[−118.8] 7.59	[−121.3] 7.51	6.8861
26					[−121.4] 7.66	[−121.5] 7.87	[−123.9] 7.79	6.9144
19				NHCH ₂ Ph	[−112.4] 6.78	[−113.3] 7.02	[−118.7] 7.23	6.9431

Table 1. (Continued)

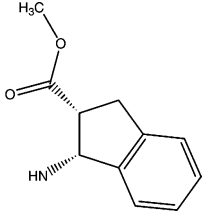
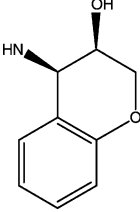
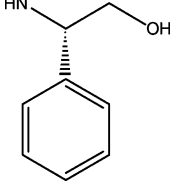
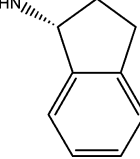
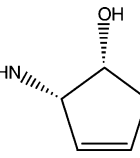
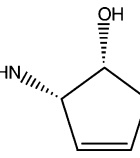
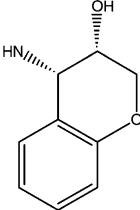
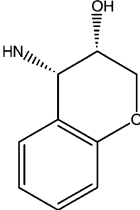
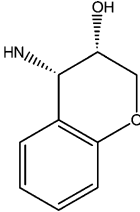
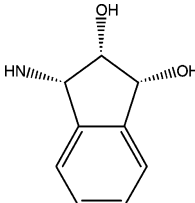
Inhibitor no.	R1	R2	R3	R4	[E_{inter}] pIC ₅₀ (calc.)			Exp. pIC ₅₀
					GROMOS	QRFF(I)	QRFF(II)	
24					[−129.7] 8.47*	[−133.0] 9.07*	[−140.8] 9.60*	7.1785
29					[−124.5] 7.97	[−126.7] 8.41	[−118.0] 7.15	7.3925
34					[−129.5] 8.46	[−114.4] 7.13	[−110.0] 6.30	7.4134
21					[−115.3] 7.06	[−113.1] 6.99	[−116.2] 6.97	7.4650
13	CH ₂ CH=CH ₂	H	H		[−123.5] 7.87	[−112.0] 6.88	[−122.6] 7.66	7.5607
20					[−118.7] 7.39	[−121.5] 7.87	[−126.6] 8.08	8.0209
3	CH ₂ Ph	CH ₃	H		[−128.7] 8.37	[−118.4] 7.55	[−127.6] 8.19	8.1135
15	CH ₂ C(O)Ph	H	H		[−139.3] 9.41*	[−141.0] 9.91	[−147.9] 10.38*	8.2660
27					[−129.0] 8.41	[−130.9] 8.85	[−137.9] 9.30	9.1549
16	CH ₂ -4-pyridyl	H	H		[−136.3] 9.12	[−138.4] 9.64	[−139.7] 9.49	9.2757
9	CH ₂ -4-NH ₂ Ph	H	H		[−143.7] 9.85	[−113.6] 7.05*	[−129.9] 8.43	9.5086
8	CH ₂ -4-CH ₃ Ph	H	H		[−134.0] 8.89	[−133.4] 9.11	[−137.0] 9.20	9.5376
5	CH ₂ -4-CF ₃ Ph	H	H		[−131.9] 8.69	[−137.2] 9.51	[−141.8] 9.72	9.5850
1	CH ₂ Ph	H	H		[−123.1] 7.83	[−127.0] 8.45	[−135.9] 9.08	9.6021
17	CH ₂ SPh	H	H		[−131.5] 8.66	[−134.1] 9.19	[−137.3] 9.24	9.6021

Table 1. (Continued)

Inhibitor no.	R1	R2	R3	R4	[E _{inter}] pIC ₅₀ (calc.)			Exp. pIC ₅₀
					GROMOS	QRFF(I)	QRFF(II)	
6	(E)-CH ₂ CH=CHPh	H	H		[-127.1] 8.22*	[-131.3] 8.90	[-123.6] 7.76*	9.6383
4	CH ₂ CH ₂ CH ₂ Ph	H	OH		[-149.7] 10.43	[-141.2] 9.93	[-149.9] 10.56	9.7212
28					[139.5] 9.44	[137.6] 9.55	[134.8] 8.97	9.7447
18	CH ₂ -4- <i>t</i> -butylPh	H	H		[136.6] 9.15	[134.5] 9.23	[139.5] 9.47	9.7696
12	CH ₂ -4-OHPh	H	H		[139.6] 9.44	[132.7] 9.04	[134.8] 8.97	9.7959
33					[142.7] 9.75	[131.5] 8.92	[143.3] 9.88	10.000

Experimental pIC₅₀ are from [8]. The ligands that were excluded from the training set are denoted by an asterisk.

Table 2. Interaction energies (kcal/mol) (ligand-protein plus ligand-water) calculated for the prediction set with different parametrizations (see text) and corresponding values of pIC₅₀.

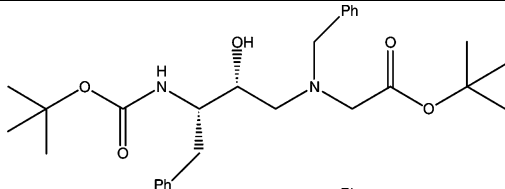
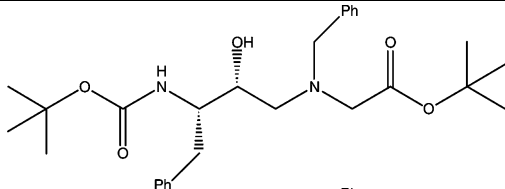
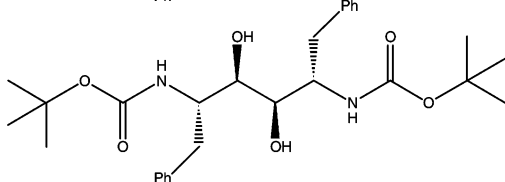
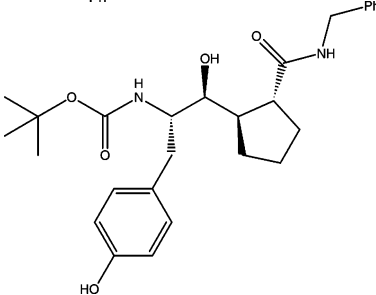
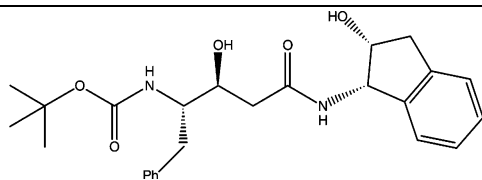
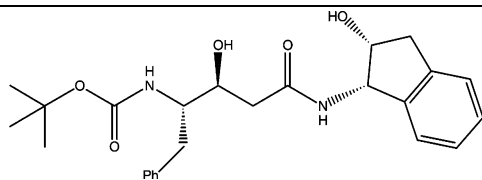
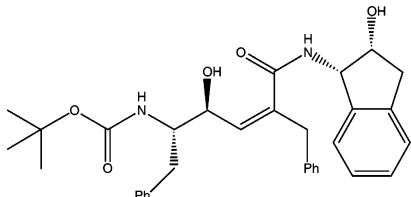
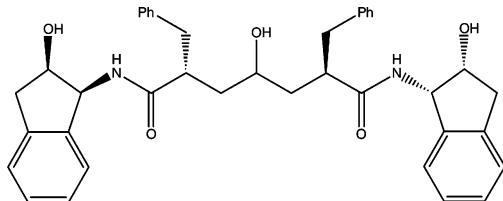
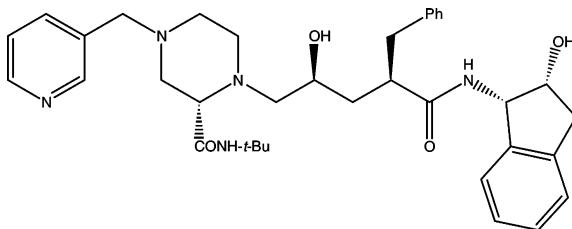
Inhibitor no.		pIC ₅₀ (calc.)	[E _{inter}] pIC ₅₀ (calc.)			Exp. pIC ₅₀
			Ref. [8]	GROMOS	QRFF(I)	
49		3.6338	[-98.2] 5.38	[-100.5] 5.67	[-102.7] 5.51	5.3279
50		3.9366	[-115.9] 7.12	[-112.4] 6.92	[-112.0] 6.51	5.8617
35		6.2760	[-116.3] 7.17	[-104.9] 6.14	[-111.1] 6.41	6.2299

Table 2. (Continued)

Inhibitor no.		pIC ₅₀ (calc.)	[E _{inter}] pIC ₅₀ (calc.)			Exp. pIC ₅₀			
			Ref. [8]	GROMOS	QRFF(I)		QRFF(II)		
37		6.3302	[-110.2]	6.57	[-113.4]	7.02	[-106.9]	5.96	6.2457
38		10.141	[-125.2]	8.04	[-130.1]	8.77	[-126.3]	8.05	8.8861
36		12.012	[-152.3]	10.69	[-142.9]	10.11	[-144.1]	9.97	9.1612
Crixivan		N. A.	[-138.4]	9.33	[-143.6]	10.18	[-149.3]	10.53	9.5229

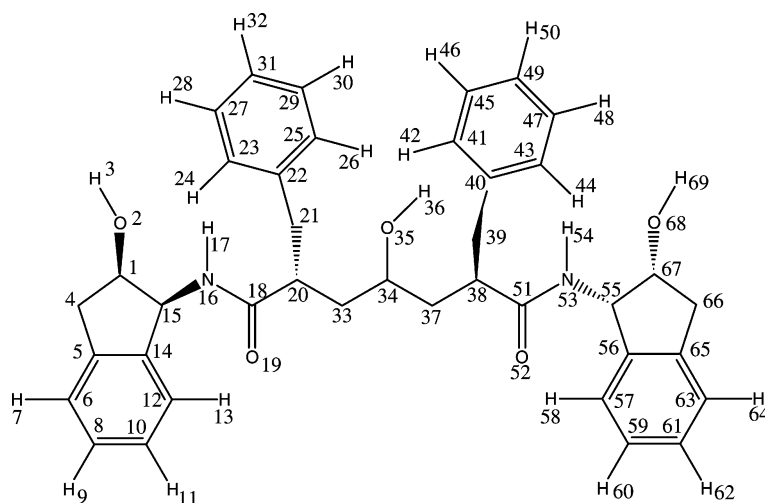
Experimental pIC₅₀ are from [8] with the exception of Crixivan from [17].

equilibration, production runs up to 1 ns were performed. In the search for a compromise between accuracy and computational effort, we checked on the convergence of the correlation coefficient for the training set and concluded that runs of the order of 100 ps were sufficient to provide the desired quantitative comparison of the different parametrizations. Subsequently, we applied the refinement procedure again to the ligand in the conformation corresponding to the final snapshot of this first phase and subjected to local energy minimization, and performed a further 50 ps run using the newly refined charges.

An example of how the atomic charges vary from one scheme to the other is given in Table 3.

Note that parameters relative to atoms belonging to functional groups that were absent in the GROMOS scheme were assigned on the basis of chemical similarity. These cases (e.g. C15 and C55 in Table 3) correspond to the largest deviation found from the GROMOS values to the quantum refined ones, which is in line with the desired action of our procedure. On the contrary, on the atoms for which the GROMOS parameters were well established (e.g. aromatic CH groups) the variations operated by the refinement tend to be modest due to the consistency restraint. Conformational changes induced by the binding can be recognized in the changes of the values of the refined charges (e.g. C34 and O35 in Table 3).

Table 3. Atomic effective charges assigned with the three different schemes for ligand no. 36 in Table 2.



Atom no.	GROMOS	QRFF(I)	QRFF(II)	Atom No.	GROMOS	QRFF(I)	QRFF(II)
C1	0.150	0.154	0.241	C67	0.150	0.195	0.187
O2	-0.548	-0.519	-0.612	O68	-0.548	-0.530	-0.592
H3	0.398	0.307	0.331	H69	0.398	0.316	0.340
C4	0.000	0.104	0.125	C66	0.000	0.041	0.051
C5	0.000	-0.018	-0.037	C65	0.000	-0.009	0.052
C6	-0.100	-0.104	-0.150	C63	-0.100	-0.134	-0.156
H7	0.100	0.100	0.096	H64	0.100	0.104	0.093
C8	-0.100	0.050	-0.100	C61	-0.100	-0.148	-0.095
H9	0.100	-0.139	0.082	H62	0.100	0.109	0.085
C10	-0.100	-0.108	-0.112	C59	-0.100	-0.071	-0.080
H11	0.100	0.101	0.087	H60	0.100	0.092	0.090
C12	-0.100	-0.173	-0.124	C57	-0.100	-0.159	-0.194
H13	0.100	0.115	0.090	H58	0.100	0.097	0.116
C14	0.000	-0.011	0.028	C56	0.000	0.051	-0.019
C15	0.000	0.215	0.197	C55	0.000	0.261	0.304
N16	-0.280	-0.449	-0.320	N53	-0.280	-0.439	-0.384
H17	0.280	0.246	0.189	H54	0.280	0.230	0.229
C18	0.380	0.447	0.402	C51	0.380	0.458	0.521
O19	-0.380	-0.451	-0.490	O52	-0.380	-0.488	-0.555
C20	0.000	0.109	0.162	C38	0.000	-0.020	-0.040
C21	0.000	0.010	0.020	C39	0.000	0.078	0.018
C22	0.000	0.094	0.031	C40	0.000	0.038	0.059
C23	-0.100	-0.130	-0.156	C43	-0.100	-0.116	-0.096
H24	0.100	0.078	0.109	H44	0.100	0.079	0.074
C25	-0.100	-0.178	-0.105	C41	-0.100	-0.119	-0.104
H26	0.100	0.109	0.078	H42	0.100	0.107	0.097
C27	-0.100	-0.081	-0.027	C47	-0.100	-0.106	-0.118
H28	0.100	0.089	0.081	H48	0.100	0.095	0.089
C29	-0.100	-0.079	-0.101	C45	-0.100	-0.127	-0.116
H30	0.100	0.090	0.085	H46	0.100	0.095	0.092
C31	-0.100	-0.115	-0.139	C49	-0.100	-0.101	-0.089
H32	0.100	0.095	0.083	H50	0.100	0.154	0.078

Table 3. (Continued)

Atom no.	GROMOS	QRFF(I)	QRFF(II)	Atom No.	GROMOS	QRFF(I)	QRFF(II)
C33	0.000	0.058	0.017	C37	0.000	0.066	0.102
C34	0.150	0.177	0.222				
O35	-0.548	-0.596	-0.657				
H36	0.398	0.304	0.332				

The sequence described above (a 100 ps run (phase I) followed by a 50 ps run (phase II)) was repeated using refined values of the effective charges also for all the residues around the binding pocket (485 atoms). As mentioned above, these were derived for the structure of the protein kept fixed in vacuum in the binding configuration.

For the sake of comparison, we have also carried out free energy calculations [18] using the multi-configuration thermodynamic integration method [19]. The number of water molecules (1483) included in the models of the ligands in pure solvent was once again chosen so as to allow at least 0.9 nm between the atoms of the ligand and the box wall. For the atoms that needed to be either created or deleted when transforming one (reference) ligand to the other, a soft-core scaling [20] was adopted for both dispersion and electrostatic interactions with soft-core parameters ranging from 0.1 to 2.0 for the former and from 0.1 to 25 for the latter. This provided the desired smoothing of the free energy curve. Depending on its shape, a number of integration points between 11 and 19 was used, which amounted to simulation times on the order of 1 ns for each leg of the cycle. This method could be applied only to 10 out of the 30 complexes of the training set (the ones labeled 4, 11, 13, 15, 21, 25, 26, 27, 30, 33 in [8]), because molecules with similar topologies are required.

Results

The evaluation of our QRFF-MD procedure is made by comparing our results for the activities of the inhibitors with experimental data, and confronting their performance with that of applications of the standard GROMOS force-field and with the original findings of [8]. First a correlation was determined (by linear regression) between the experimental activities of the 30 compounds of the training set and their interaction energies with the enzyme, obtained averaging over the simulation

Table 4. Correlation between computed and experimental pIC_{50} values: root mean square deviations (rmsd) obtained for the training (A) and prediction (B) sets using different methods.

Ref. [8]	GROMOS	QRFF(I)	QRFF(II)
(A) 0.82	0.79	0.74	0.63
(B) 1.20/-	0.90/0.84	0.68/0.68	0.57/0.65

In (B), the values on the right correspond to the set including Crixivan.

runs. In each case, we excluded the few (5 or 6) data points corresponding to an error greater than 1.5 and determined a new correlation.² This pruning procedure was adopted in order to avoid large errors in the training set due to factors that were not under control in this kind of simulations; for example, those caused by a wrong initial pose of the ligand or suboptimal force-field parameters, and those pertaining to the experimental data. Then we applied the new correlation to predict the inhibitor activity of a new set of ligands, as done in [8]. Note that the ligands of the prediction set are conceptually different from the ones included in the training set because they were specifically designed to solve structural questions or pharmacokinetic properties.

The outputs of those calculations are reported in Tables 1, 2 and 4, where the consistent quantum refinement of the electrostatics refers only to the ligands. In particular, we now consider Table 4 where the root-mean-square-deviation (rmsd) of the pIC_{50} estimates are given. In the case of the training set (Table 4A), comparison with Ref. [8] shows that our two-step procedure (QRFF(II))

²Note that for a consistent comparison of our results with those of [8] we recalculated the correlation of the training set using the same inhibitors as in our training set and also discarded all inhibitors that exhibited an error in pIC_{50} larger than 1.5. This procedure was also carried out for the data obtained using both the native and the L-689,502 inhibited HIV-1 protease structures of [8]. The predictions from [8] were then recalculated using these corrected training sets.

gives remarkably better results. The effect of the iterated refinement, namely the difference between phase I and phase II, is relevant, showing that there was a non-negligible dependence of the effective charges on the atomic configuration and that this had changed significantly after 100 ps. One should, however, note that our starting configurations were adjusted manually so that the 100 ps MD run was necessary for the rearrangement of the complex in the binding configuration; this time can be avoided – and thus the iterative refinement – if the result of an educated docking is taken as the initial configuration. We have verified that for the systems considered here, a longer run did not change the results appreciably. Moreover, we have assessed the significance of the improvements obtained on the binding energy estimations by means of statistical analysis. The value of the correlation coefficient R^2 , the cross-validated R^2 and the root-mean-square-error of validation (RMSEv) are $R^2=0.59$, cross-validated $R^2=0.53$ and RMSEv=0.85 for GROMOS, $R^2=0.63$, cross-validated $R^2=0.57$ and RMSEv=0.80 for QRFF(I), and are $R^2=0.74$, cross-validated $R^2=0.69$ and RMSEv=0.70 for QRFF(II). In each case, the fact that R^2 and cross-validated R^2 are comparable indicates that the model is pre-

dictive and that there is no bias in the training set obtained after pruning. The coefficients (a,b) in the derived regression equations $\text{pIC}_{50} = a \cdot E_{\text{inter}} - b$ are $(-0.09798; 4.2333)$, $(-0.10444; 4.81757)$ and $(-0.10776; 5.56110)$ for the GROMOS, QRFF(I) and QRFF(II) training sets, respectively.

When considering the prediction set, the advantage obtained with our method is more pronounced (Table 4B). Moreover, although the quality of the correspondence between theory and experiment is the same for the training and the prediction sets in the case of the QRFF-MD methodology, a substantial decrease in the performance is shown by the GROMOS-MD and also in [8]. This difference can be regarded as a consequence of the greater flexibility of our procedure, which better accounts for the diversity of the two sets of ligands. Note in particular that the most remarkable outlier found in Ref. 8 (ligand no. 36 in Table 3) is not an exceptional case in our prediction scheme (see Table 2). As mentioned above, our prediction set includes indinavir sulphate – which was not in the original set of [8]. It is significant that its high activity [17] is correctly predicted by our method (Figure 1).

The results obtained when the residues around the active site were also represented with the

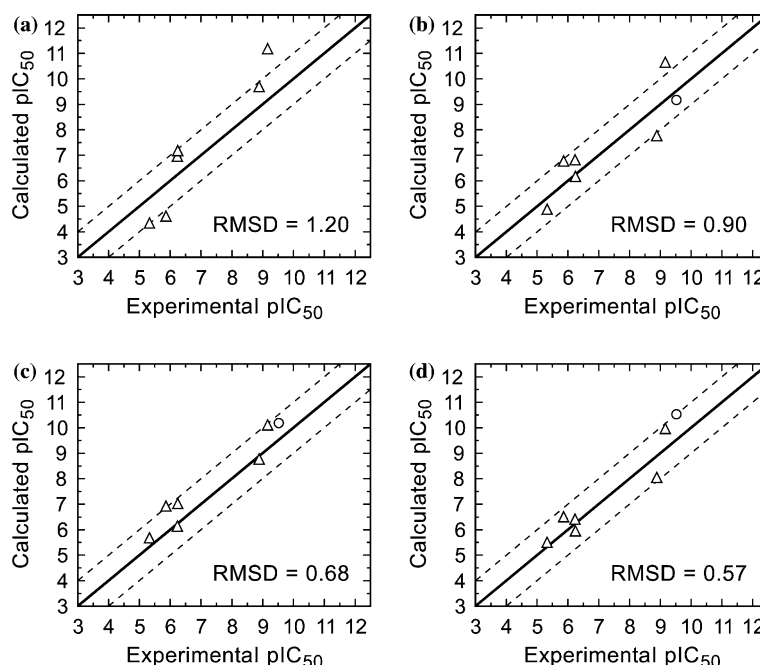


Figure 1. Predictions vs. experimental data for the activities of HIV-1 protease inhibitors: from (a) [8], (b) GROMOS-MD, our QRFF-MD after (c) the first (phase I) and (d) second (phase II) refinement. Circles correspond to Crixivan.

QRFF do not show an improvement: the rmsd resulting for the training set was 0.70 and 0.72 for the first and second phases, respectively. Clearly, it is not worth the additional computational cost. Indeed the electrostatic parameters for the protein are already optimized in the original force field, and our refinement imposes the specificity of the electrostatics of one binding configuration, which may not be suitable for the others. Reiterated refinement also for the charges of the atoms in the binding pocket would be the most direct solution, but this does not seem viable because the increase in computational cost is not compensated by the expected gain.

Correlations based on free energies are in principle more appropriate than those based on interaction energies but clearly computationally much more costly. Our aim here was to determine to what extent the gain in accuracy was worth it. Our investigation was, however, restricted to only 10 out of the 30 inhibitors of the training set by necessity. The value of the rmsd relative to this limited set decreased by 0.2 and 0.3 for GRO-MOS-MD and QRFF-MD, respectively. Such an improvement, although significant as expected, does not offset the drawback of the method, namely its intrinsic limitation to a subset of similar compounds and the computational cost, which is one order of magnitude higher than that required by the procedure described in this article. On the contrary, the enhancement obtained by introducing a consistent quantum refinement to the force field entails an additional computational cost that is only a negligible fraction of the simulation time. Indeed the time required for the refinement of the potential on a typical ligand (~ 100 atoms) is of the order of 1 min, whereas the time required to generate a 50 ps MD trajectory is of the order of 1 h (on a IBM p690 32-way hardware).

Conclusions

Molecular dynamics simulations can offer an attractive tool for the search of novel lead compounds, but the accuracy of the force-field modeling of the interatomic interactions is crucial to grant their validity. By introducing selected and accurate information from quantum mechanical calculations one can in principle ameliorate the description of interatomic interactions provided

by the force fields commonly used in molecular mechanics/dynamics calculations of ligand–protein complexes. We have proposed a novel methodology for such a refinement that uniquely satisfies internal consistency requirements of the force field. Here we have applied it to the GRO-MOS force field to ameliorate the modeling of the electrostatic terms of the ligand–protein interaction. The test we have chosen for the validation of our global procedure (two-step QRFF-MD) was on the prediction of the activity of a set of HIV-1 protease inhibitors. Although the binding to the active site of HIV-1 protease represents a particularly hard test case,³ the results are encouraging because a clear improvement has been found compared with previous molecular mechanics calculations [8] and also with MD using the original reference force field.

Extension to other protein–ligand complexes and application to other force fields will be the next steps of this research. For example, given that the correct description of a hydrogen bond crucially depends on the carefully balanced parameterization of dispersion and electrostatic interaction terms, we expect to obtain a more substantial improvement for cases where hydrogen bonds play a dominant role in the ligand–protein binding. Moreover, quantum calculations similar to those we have performed to extract refined values for the effective charges can be used to derive more accurate parameters for other interaction terms, provided that global consistency is maintained. For example, this was the case in our study of progesterone, for which an accurate account of the torsional potential was needed [7].

Clearly the reach of our proposed methodology can be further extended by using common techniques of MD to enhance the conformational sampling [22], and also coupled to efficient approximations of free energies like the linear interaction energy (LIE) method [23]. Given that accurate free energy computations are still unaffordable and that full *ab initio* calculations, which would be desirable for an unbiased and unrestrained representation for

³It is well known [21] that all classical force fields have an intrinsic difficulty to represent the angle between the two catalytic aspartates measured in the crystallographic structures of the complexes. In the case of the GRO-MOS force field, the value we obtained from averaging over the simulation runs ranges between 40° and 77°, depending on the specific complex, whereas experimental data lie around 20°.

the ligand–protein complexes, are prohibitively expensive, we regard our two-step QRFF-MD as representing a good compromise in terms of both accuracy and speed performance.

References

1. Lyne, P.D., *Drug Discov. Today*, 7 (2002) 1047.
2. Gohlke, H. and Klebe, G., *Angew. Chem. Int. Ed. Engl.*, 41 (2002) 2644.
3. McConkey, B.J., Sobolev, V. and Edelman, M., *Curr. Sci.*, 83 (2002) 845.
4. Parr, R.G. and Yang, W., *Density Functional Theory of Atoms and Molecules*. Oxford University Press, New York, 1989.
5. CPMD V3.7 Copyright IBM Corp. 1990–2003, Copyright MPI für Festkörperforschung Stuttgart 1997–2001. See <http://www.cpmd.org>.
6. (a) Momany, F., *J. Phys. Chem.*, 82 (1978) 592; (b) Singh U.C. and Kollman, P.A., *J. Comput. Chem.*, 5 (1984) 129.
7. Mordasini, T., Curioni, A., Bursi, R. and Andreoni, W., *ChemBioChem*, 4 (2003) 155.
8. Holloway, M.K., Wai, J.M., Halgren, T.A., Fitzgerald, P.M.D., Vacca, J.P., Dorsey, B.D., Levin, R.B., Thompson, W.J., Chen, L.J., deSolms, S.J., Gaffin, N., Ghosh, A.K., Giuliani, E.A., Graham, S.L., Guare, J.P., Hungate, R.W., Lyle, T.A., Sanders, W.M., Tucker, T.J., Wiggins, M., Wiscount, C.M., Woltersdorf, O.W., Young, S.D., Darke, P.L. and Zugay, J.A., *J. Med. Chem.*, 38 (1995) 305.
9. van Gunsteren, W.F., Billeter, S.R., Eising, A.A., Hünenberger, P.H., Krüger, P., Mark, A.E., Scott, W.R.P. and Tironi, I.G. *Biomolecular Simulation: The GROMOS96 Manual and User Guide*, vdf: Hochschulverlag AG an der ETH Zürich and BIOMOS B.V., Zürich, Switzerland, Groningen, The Netherlands, 1996, ISBN 3 7281 2422 2.
10. Berendsen, H.J.C., Postma, J.P.M., van Gunsteren, W.F. and Hermans, J., In Pullman, B. (Ed.), *Intermolecular Forces*. Reidel, Dordrecht, The Netherlands, 1981, pp. 331–342.
11. Troullier, N. and Martins, J.L., *Phys. Rev. B*, 43 (1991) 1993.
12. Bayly, C.I., Cieplak, P., Cornell, W.D. and Kollman, P.A., *J. Phys. Chem.*, 97 (1993) 10269.
13. Becke, A.D., *Phys. Rev. A*, 38 (1988) 3098.
14. Lee, C., Yang, W., Parr, R.G., *Phys. Rev. B*, 37 (1988) 785.
15. Pearlman, D.A., Case, D.A., Caldwell, J.W., Ross, W.S., Cheatham, III, T.E., DeBolt, S., Ferguson, D., Seibel, G. and Kollman, P., *Comp. Phys. Commun.*, 91 (1995) 1.
16. Fitzgerald, P.M.D., McKeever, B.M., Van Middlesworth, J.F., Springer, J.P., Heimbach, J.C., Leu, C.-T., Herber, W.K., Dixon, R.A.F. and Darke, P.L., *J. Biol. Chem.*, 265 (1990) 14209.
17. Lin, J.H., Ostovic, D. and Vacca J.P., In Borchardt, R.T. et al. (Eds.), *Integration of Pharmaceutical Discovery and Development: Case Studies*. Plenum Press, New York, 1998, Chapter 11, pp. 233–255.
18. van Gunsteren, W.F., In van Gunsteren, W.F. and Weiner P.K. (Eds.), *Computer Simulation of Biomolecular Systems, Theoretical and Experimental Applications*. Escom Science Publishers, Leiden, The Netherlands, 1989, pp. 27–59.
19. Straatsma, T.P. and McCammon, J.A. J., *Chem. Phys.*, 95 (1991) 1175.
20. Beutler, T.C., Mark, A.E., van Schaik, R.C., Gerber, P.R. and van Gunsteren, W.F., *Chem. Phys. Lett.*, 222 (1994) 529.
21. Hodge, C.N., Straatsma, T.P., McCammon, J.A. and Wlodawer, A., In Chiu, W., Burnett, R.M. and Garcea, R. (Eds.), *Structural Biology of Viruses*. Oxford University Press, New York, 1997.
22. Taylor, R.D., Jewsbury, P.J. and Essex J.W., *J. Comput.-Aided Mol. Des.*, 16 (2002) 151.
23. Zhou R., Friesner, R.A., Ghosh, A., Rizzo, R.C., Jorgensen, W.L. and Levy, R.M., *J. Phys. Chem.*, 105 (2001) 10388; Zoete, V., Michielin O. and Karplus M., *J. Comput.-Aided. Mol. Des.*, 17 (2003) 861.